Molecules and Cells

Interleukin-9 Inhibits Lung Metastasis of Melanoma through Stimulating Anti-Tumor M1 Macrophages

Sang Min Park[1], Van Anh Do-Thi[1], Jie-Oh Lee[2], Hayyoung Lee[3,*], and Young Sang Kim[1,*]

[1]Department of Biochemistry, College of Natural Sciences, Chungnam National University, Daejeon 34134, Korea, [2]Department of Life Sciences, POSTECH, Pohang 37673, Korea, [3]Institute of Biotechnology, Chungnam National University, Daejeon 34134, Korea
*Correspondence: young@cnu.ac.kr (YSK); hlee@cnu.ac.kr (HL)
https://doi.org/10.14348/molcells.2020.0047
www.molcells.org

Interleukin-9 (IL-9) is well known for its role in allergic inflammation. For cancer, both pro- and anti-tumor effects of IL-9 were controversially reported, but the impact of IL-9 on tumor metastasis has not yet been clarified. In this study, IL-9 was expressed as a secretory form (sIL-9) and a membrane-bound form (mbIL-9) on B16F10 melanoma cells. The mbIL-9 was engineered as a chimeric protein with the transmembrane and cytoplasmic region of TNF-α. The effect of either mbIL-9 or sIL-9 expressing cells were analyzed on the metastasis capability of the cancer cells. After three weeks of tumor implantation into C57BL/6 mice through the tail vein, the number of tumor modules in lungs injected with IL-9 expressing B16F10 was 5-fold less than that of control groups. The percentages of $CD4^+$ T cells, $CD8^+$ T cells, NK cells, and M1 macrophages considerably increased in the lungs of the mice injected with IL-9 expressing cells. Among them, the M1 macrophage subset was the most significantly enhanced. Furthermore, peritoneal macrophages, which were stimulated with either sIL-9 or mbIL-9 expressing transfectant, exerted higher anti-tumor cytotoxicity compared with that of the mock control. The IL-9-stimulated peritoneal macrophages were highly polarized to M1 phenotype. Stimulation of RAW264.7 macrophages with sIL-9 or mbIL-9 expressing cells also significantly increased the cytotoxicity of those macrophages against wild-type B16F10 cells. These results clearly demonstrate that IL-9 can induce an anti-metastasis effect by enhancing the polarization and proliferation of M1 macrophages.

Keywords: anti-cancer, B16F10 melanoma, cytokine, immunotherapy, interleukin-9

INTRODUCTION

Interleukin-9 (IL-9) was at first characterised as a growth factor for mast cells and T cells (Goswami and Kaplan, 2011). Although the primary source of IL-9 is a subset of T lymphocytes called Th9, the other T cells subsets such as Th2, Th17, or Treg also can express IL-9 (Dardalhon et al., 2008; Goswami and Kaplan, 2011). IL-9 production can be induced by cytokines such as IL-1β, IL-2, IL-4, IL-6, IL-9, IL-10, IL-12, TGF-β, or inhibited by IFN-γ (Lee et al., 2019). The two transcription factors, PU.1 and IRF4, are responsible for IL-9 production (Chang et al., 2010; Mudter et al., 2008). IL-9 exerts its effect by binding to the IL-9 receptor complex (IL-9R). IL-9Rα, a receptor subunit with high affinity for IL-9, forms a heterodimeric receptor complex with a signaling subunit, common gamma (γc) chain (Chakraborty et al., 2019). Although both secretory and membrane-bound form of IL-9Rα are found,

Received 17 Feburary, 2020; revised 23 March, 2020; accepted 6 April, 2020; published online 24 April, 2020

eISSN: 0219-1032

the possibility of IL-9Rα to form the complex with the γc subunit is low. After binding to IL-9, the percentage to form the receptor complex is accelerated (Chakraborty et al., 2019; Malka et al., 2008).

IL-9 exerts its multifunctional effects via direct or indirect ways in immune cells such as lymphocytes, Treg cells, and hematopoietic progenitor cells, or non-immune cells such as airway smooth muscle cells, epithelial cells (Goswami and Kaplan, 2011; Lee et al., 2019). The role of IL-9 in the inflammation condition has been robustly reported. High levels of IL-9 is related to allergy and autoimmune disease (Ciccia et al., 2015; Dantas et al., 2015; Li et al., 2011; Nalleweg et al., 2015). The potent role of IL-9 in inducing immune tolerance was also reported. However, the role of IL-9 in the pathogenesis of cancer is still controversial. On the one hand, the pro-tumor effect of IL-9 in leukemia, lymphoma, breast cancer, lung cancer, thyroid cancer, colon cancer was reported (Lee et al., 2019). On the other hand, the anti-tumor effect of IL-9 in melanoma, lung adenocarcinoma, breast cancer, and colon cancer was also shown (Do Thi et al., 2018; Fang et al., 2015; Wang et al., 2019; You et al., 2017). The conflicting results among different cancer cells in various conditions imply the pleiotropic characteristics of IL-9.

In this study, to clarify the above assumption, the effect of membrane-bound form (mbIL-9) or secretory form (sIL-9) of IL-9 overexpression on B16F10 melanoma, an IL-9R expressing cancer cell line, was investigated. Although overexpression of IL-9 or treatment with soluble IL-9 promoted the proliferation and migration of B16F10 cells *in vitro*, the ectopic expression of IL-9 reduced tumor growth and inhibited the metastasis capability of the transfectants in mice. The IL-9 released from the transfectants triggered anti-tumor response indirectly through stimulating both innate (NK, macrophage) and adaptive immune response ($CD4^+$, $CD8^+$ T lymphocytes) *in vitro* and *in vivo*. Here, we provide the first evidence to show that IL-9 exerts an anti-metastasis effect by enhancing polarization and proliferation of M1 macrophage.

MATERIALS AND METHODS

Tumor cell line and mice

Female C57BL/6JBomTac mice were obtained from Daehan Biolink (Eumseong, Korea), and all mice were used between 6 and 8 weeks of age. All animal procedures were approved and guided by the Institutional Animal Care and Use Committee (IACUC) of Chungnam National University (CNU-01056). The murine melanoma B16F10 and macrophage RAW264.7 cells were cultured in DMEM (Gibco, USA) supplemented with 10% heat-inactivated fetal bovine serum (FBS; Gibco), 2 mM L-glutamine, 100 U/ml penicillin, 100 μg/ml streptomycin (Sigma, USA) in humidified 5% CO_2 at 37°C. G418 (Santa Cruz Biotechnology, USA) was used as a selective agent for transfections.

Antibodies and reagents

Anti-mouse IL-9 polyclonal antibody (504802), FITC-goat anti-hamster (Armenian) IgG (405502) and APC-rat anti-mouse CD49b were purchased from Biolegend (USA). PE-rat anti-mouse CD4 (553730), purified rat anti-mouse CD8a (553027), PE-mouse anti-rat IgG, purified hamster anti-mouse CD3 (557306), FITC-mouse anti-hamster (Armenian) IgG (554008) and PE-mouse anti-mouse NK1.1 (557391) were purchased from BD Biosciences (USA). Anti-L^d MHC class I (28-14-8S), FITC-goat anti-mouse IgG (sc-2005) were purchased from Santa Cruz Biotechnology. PE-hamster (Armenian) anti-mouse CD80 (12-0801-81), PE-rat anti-mouse CD86 (12-0862-82) and APC-rat anti-mouse F4/80 (17-4801-82) were purchased from Thermo Fisher Scientific (USA). Recombinant mouse IL-9 was purchased from Komabiotech (Korea).

Plasmid construction and transfection

Insert cDNAs of sIL-9 and mbIL-9 were cloned in the pcDNA3.1(+) plasmid as previously described (Do Thi et al., 2016). B16F10 melanoma cells were stably transfected with the plasmid DNA or empty vector using Lipofectamine 2000 (Thermo Fisher Scientific). After 18 h, the cells were plated in 96-well plates using 1 mg/ml G418-containing medium. Drug-resistant colonies were usually visible after 2 weeks. Transfectants expressing sIL-9 and mbIL-9 were selected by semi-quantitative reverse transcription polymerase chain reaction (RT-PCR) using primers described in Supplementary Table S1.

ELISA for IL-9

The concentration of IL-9 was quantitated using IL-9 ELISA kit (Biolegend). Transfectants (2×10^5 cells/clone) were incubated in 3 ml of culture medium in 6-well culture plates at 37°C for 72 h. Then culture supernatants were separated and subjected to ELISA assay following the instruction of the manufacturer. To analyse the IL-9 secreting ability of mitomycin C (MMC)-inactivated tumor clones, 1×10^6 MMC-treated sIL-9 cells were seeded in the 24-well plate. As a control, 1×10^6 non-treated sIL-9 cells were seeded at the same time in the same plate. After 24 h incubation, the culture supernatants were collected and examined by ELISA. Since MMC-treated cells cannot proliferate, the amount of IL-9 released by the treated sIL-9 cells was normalized by the ratio of cell numbers of the treated versus non-treated sIL-9 cells.

Flow cytometry analysis

For fluorophore-conjugated antibodies, cells were stained with either antigen-specific antibody or isotype control antibody. For non-conjugated antibodies, cells were stained via two steps. Firstly, cells were incubated with a diluted primary antibody. After washing off the unbound antibody, the cells were stained with fluorophore-conjugated secondary antibody. All antibodies were diluted in staining buffer (1× phosphate-buffered saline [PBS] containing 0.02% sodium azide and 2% FBS), and each staining step lasted for 1 h at 4°C in the dark. For carboxyfluorescein succinimidyl ester (CFSE) staining, cells incubated with 2.5 μM CFSE for 20 min, and the CFSE labelled cells were analysed by a flow cytometer (FACS Calibur or FACS Canto; BD Biosciences).

Cell proliferation assay

To analyze the proliferation of transfected cells, 1×10^4 cells of each clone were seeded on a 96-well plate and the cell

proliferation was analysed with MTT (3-(4,5-dimethylthiazol-2-yl)-2,5-diphenyltetrazolium bromide) assay (DyneBio, Korea). For CFSE proliferation assay, 1×10^5 CFSE labelled transfected cells were seeded in 12-well plate. The fluorescent signal was analysed by FACS after indicated time periods. To collect soluble IL-9, the supernatants from sIL-9 transfected cells cultured for 72 h were harvested and stored at −72°C. Effect of soluble IL-9 from culture supernatant on wild-type B16F10 was examined by treatment with the culture supernatant of the transfectant in 3-fold dilution using medium.

Cell cycle analysis

The cell cycle was analyzed with a flow cytometer (FACS Calibur) using propidium iodide (PI; Sigma). Briefly, 2×10^5 transfected cells were seeded on 6-well plates. After 48 h, the cells were harvested and fixed in 70% ethanol at −4°C for 1 h. The cells were twice washed with PBS and then stained with a staining solution containing PI (50 μg/ml) and RNase A (100 μg/ml) for 20 min.

Wound healing assays

To analyze the migration capability of tumour cells, transfected B16F10 cells were grown at 70% to 80% confluence in 6-well plate and scratched with yellow pipette tips. The scratch wounds were photographed by phase-contrast microscope (TS100; Nikon, Japan) every 12 h. The closed wound areas were quantitated by Adobe Photoshop CS6 software (Adobe Systems, USA).

Transwell migration assay

A Transwell chamber (pore size of 8.0 μm; SPL, Korea) was used as the upper chamber to seed 5×10^4 transfected cells in 300 μl of serum-free DMEM. A 24-well plate was used as a lower chamber containing 750 μl of complete DMEM medium. After assembling of chambers, cells were cultured in a humidified 5% CO_2 at 37°C for 48 h or 72 h. After incubation, non-invaded cells were scraped off with a cotton swab. The translocated cells on the bottom of the upper chamber membrane were fixed with 3.7% formaldehyde and stained with 2% crystal violet. Five fields of fixed cells were randomly chosen and counted under a phase-contrast microscope (TS100).

Tumor challenge

For tumorigenicity studies, syngeneic C57BL/6 mice were injected subcutaneously (right flank) with 5×10^4 live cells in 0.1 ml PBS, and tumor growth and survival was monitored daily. Tumor size was measured with a caliper and tumor volume was calculated according to the following formula: $0.52 \times S^2 \times L$, where L is the length and S is the width of the tumor. Bodyweight was also monitored daily. As controls, C57BL/6 were challenged with wild-type or mock vector-transfected B16F10 cells. For lung metastasis experiments, 5×10^4 B16F10 transfected cells in 0.2 ml PBS were injected intravenously through the lateral tail vein. After 18 days, mice were sacrificed and the metastasis nodules on lung were counted.

Peritoneal macrophage isolation

Female C57BL/6 mice were sacrificed, and 5 ml of PBS was injected into the peritoneal cavity of the mice. After brief gentle massage for 5 min, the ascitic fluid was carefully collected using a 5 ml syringe. After centrifugation at 1,500 rpm for 8 min, the pellets were re-suspended in 1 ml of complete DMEM. After 18 h incubation, non-adherent cells were removed by washing off with PBS.

Cytotoxicity assay

The cytotoxicity assay of splenic cells was performed as described previously (Do Thi et al., 2019). For the cytotoxicity assay of RAW264.7 macrophage, RAW264.7 cells were stimulated by co-culturing with each MMC-inactivated transfected B16F10 clones at a 1:1 ratio for 24 h. Then, effector cells and CFSE-labelled target cells were mixed at a 4:1 ratio. After 4 h, cells were harvested, and the apoptosis cells were stained with PI. Percentage of $CFSE^+$ and PI^+ cells were analyzed (FACS Canto). For the cytotoxicity assay of peritoneal macrophages, *ex vivo* macrophages were cultured overnight. After the removal of lymphocytes by discarding the suspension cells, the MMC-treated transfectants were added at a 1:1 ratio for co-culture. After 24 h, the CFSE-labelled B16F10 was added at a ratio of 4:1 (effector:target). After 4 h, cells were harvested, and stained with PI. Percentage of $CFSE^+$ and PI^+ cells were analysed with FACS Canto.

Statistical analysis

All data were presented as mean ± SEM (error bars). GraphPad Prism 5 (GraphPad Software, USA) was used to analyze one-way or two-way ANOVA to point out significant differences between groups ($*P < 0.05$, $**P < 0.01$, $***P < 0.001$).

RESULTS

Generation of tumor clones expressing sIL-9 or mbIL-9

The sIL-9 expression vector encodes a natural IL-9 containing IL-9 signal peptide and the functional IL-9 domain (Fig. 1A). The mbIL-9 is a chimeric protein containing cytoplasmic and transmembrane domains from TNF-α, and the complete functional IL-9 domain, as previously reported (Do Thi et al., 2018). B16F10 melanoma cells were stably transfected by the vectors of mock, sIL-9, and mbIL-9 and selected in G418-containing medium. Notably, the parent B16F10 cells did not express endogenous IL-9 at mRNA level, and the clone of sIL-9 secreted IL-9 protein up to 1,300 pg/ml (by 2×10^5 cells in 72 h) as measured in ELISA (Figs. 1B and 1C). MMC is an antitumor drug that can permanently inhibit cell division due to its stable cross-linking with nucleus DNA. The MMC-treated cells, however, persist the cellular morphology and secretion of cytokine for several days. As shown in Fig. 1D, MMC-treated sIL-9 cells released IL-9 in a comparable amount to the non-treated cells. The presence of membrane-bound IL-9 on the cell surface of mbIL-9 transfectant was selected by RT-PCR and confirmed by flow cytometry (Fig. 1E).

The biological effect of the chimeric mbIL-9 was evaluated by their capability to promote the proliferation of splenocytes. As shown in Fig. 1F, when the mice splenocytes were co-cul-

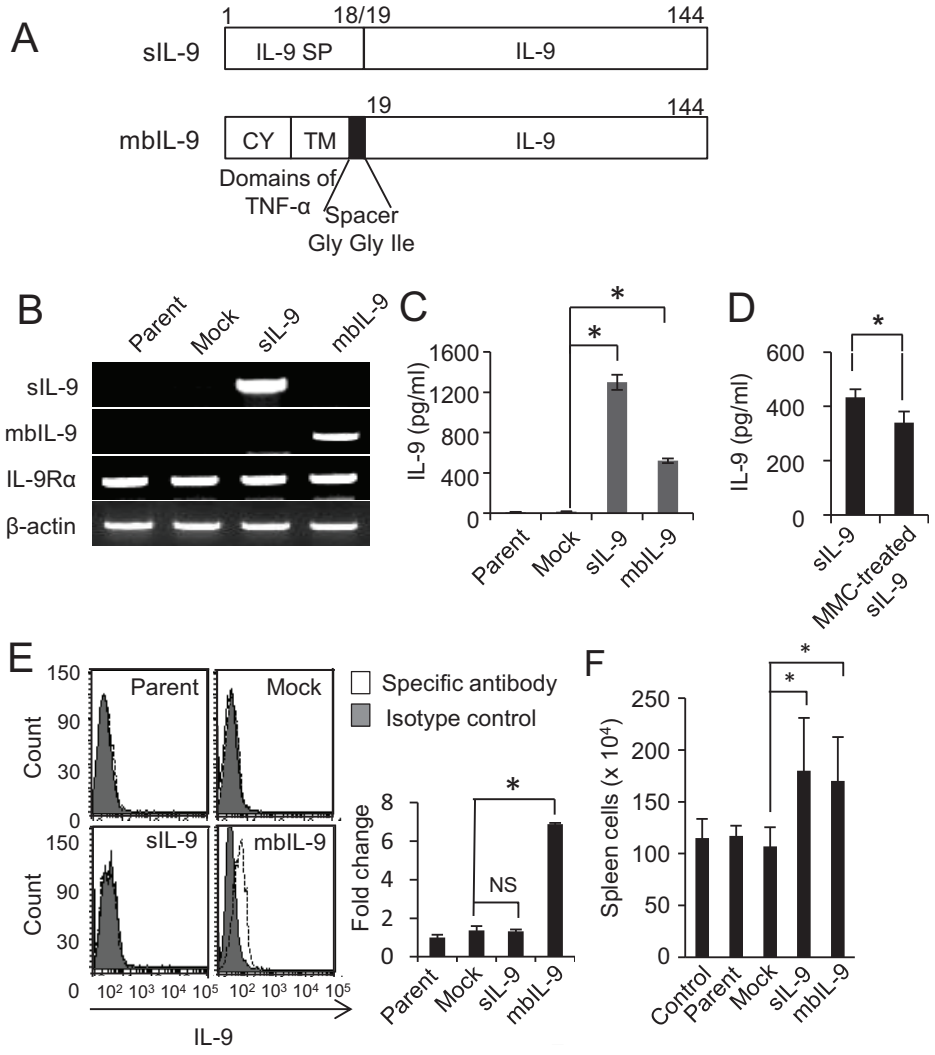

Fig. 1. Generation of B16F10 tumor clones stably expressing sIL-9 and mbIL-9. (A) The sIL-9 was comprised of IL-9 signal peptide and the complete functional IL-9 domain. The chimeric mbIL-9 composed of the cytoplasmic domain (from -75 to -45 amino acids, CY), transmembrane fragment (from -44 to -24 amino acids, TM) of murine TNF-α and the IL-9 domain (19-144 amino acids). A spacer sequence (Gly-Gly-Ile) was inserted between TNF-α and IL-9. (B) Verification of IL-9 and IL-9Rα expression in transfected clones by RT-PCR. All experimental groups expressed IL-9 receptor at mRNA level. (C) Quantitation of soluble IL-9 from the media of 2×10^5 cells of each transfectant after culturing for 72 h by ELISA. (D) Comparison of IL-9 releasing capability between the live and MMC-inactivated sIL-9 cells after culturing for 24 h. (E) The surface expression of IL-9 was analyzed by flow cytometry after staining with the polyclonal anti-IL-9 antibody. (F) Splenocytes were co-cultured with either parent or each transfected clone. After 72 h, viable splenocytes were counted by trypan blue exclusion. Control is the splenocytes without co-culture. All data were presented as mean ± SEM. $*P < 0.05$, NS, not significant.

tured with the MMC-treated stably transfected B16F10, both sIL-9 and mbIL-9 produced by each clone stimulated the proliferation of spleen cells.

IL-9 promoted the proliferation and migration of B16F10 cells *in vitro*

As shown in Fig. 1B, B16F10 melanoma cells express a moderate level of the endogenous receptor of IL-9, IL-9Rα. Therefore, we examine the direct effect of sIL-9 and mbIL-9 on the cell growth of the B16F10 clones. The MTT assay was performed to compare the proliferation rate among the transfectants. Ectopic expression of either sIL-9 or mbIL-9 exerted the direct autocrine effect on B16F10 transfectants by fastening their proliferation rate in 1.6-fold after 48 h (Fig. 2A). To confirm that IL-9 served as a growth factor for B16F10 tumor cells, the change in the proliferation rate of wild-type B16F10 after treated with soluble IL-9 was analysed by MTT. After treating with culture supernatant of sIL-9 clone, containing soluble IL-9, the proliferation of wild-type B16F10 increases 1.4-fold after 48 h (Fig. 2B), which is a consistent result with Fig. 2A. To analyze whether the increased viable cells are originated from enhanced proliferation, we performed

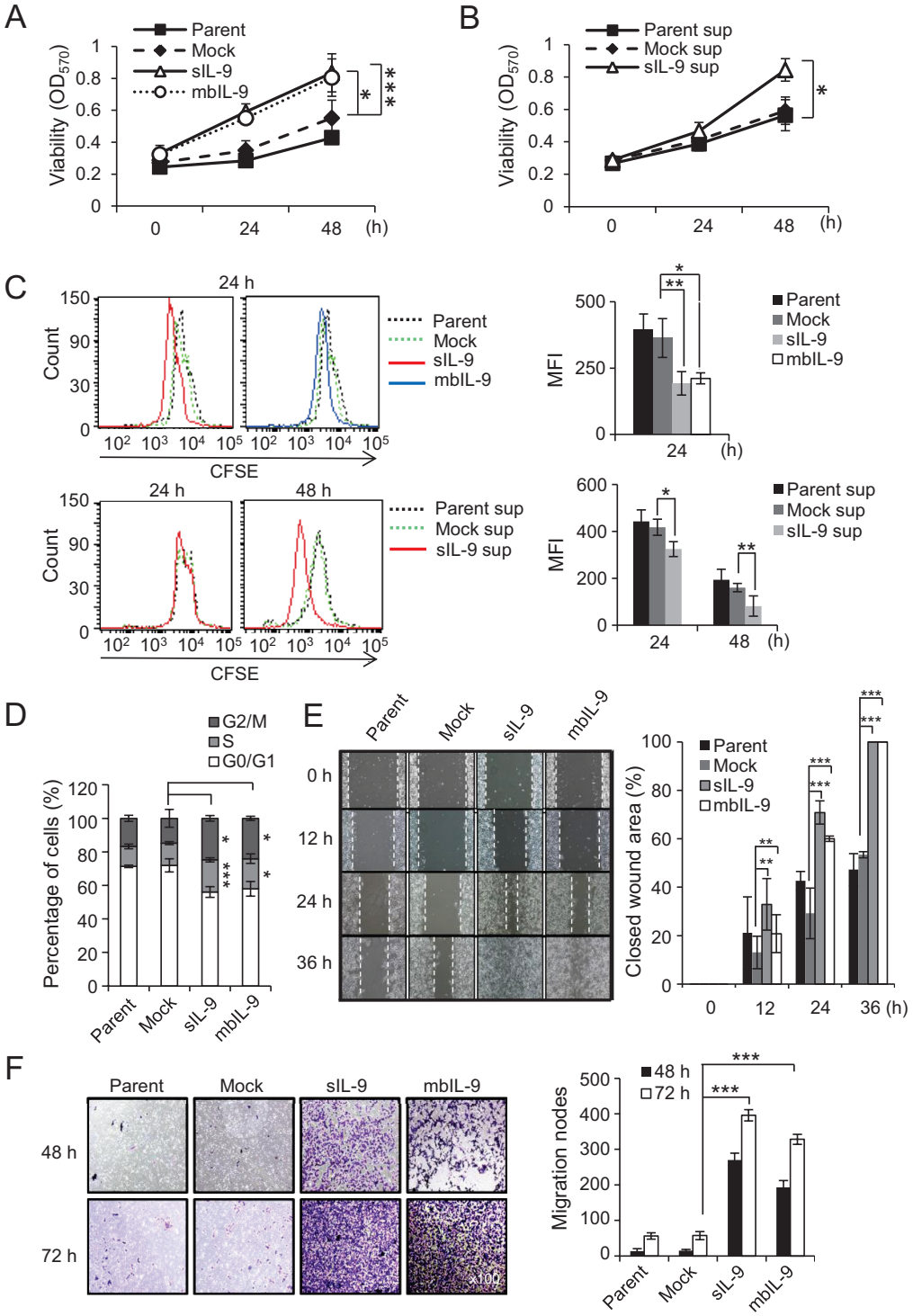

Fig. 2. Autocrine effect of IL-9 on the *in vitro* proliferation and migration of B16F10 cells. (A) The proliferation rates of control, sIL-9 and mbIL-9 expressing cells were analyzed by MTT assay. (B) The proliferation rates of wild type of B16F10 cells were analyzed after treatment with culture supernatant containing soluble IL-9. (C) The proliferation rate of the cells was analyzed by CFSE-staining. The diminished fluorescence was monitored by flow cytometry after 24 and 48 h. The mean fluorescence intensity (MFI) was shown as the bar graphs. (D) Cells were stained with PI and were examined by flow cytometric cell cycle analysis. Cell cycle distributions were analyzed with ModFit LT software. (E) Cell migration was examined by wound healing assay. The images were taken in 12-h intervals and the percentages of migration were graphed. (F) After transwell migration assay, cells were stained with crystal violet solution (×100), photographed and counted manually. The number of migration nodes was presented in the bar graph. All data were presented as mean ± SEM (error bars). $*P < 0.05$, $**P < 0.01$, $***P < 0.001$.

CFSE-staining and cell cycle analysis. CFSE is a common dye used in a cell proliferation assay. As CFSE enters viable cells, it covalently binds with amino groups of proteins to convert to fluorescent forms. Since CFSE stably links to protein, its fluorescence will be gradually reduced a half when cells divide. After staining with CFSE for 24 h, the fluorescence from sIL-9 or mbIL-9 transfectants reduced 1.7~1.9-fold compared to those from control groups (Fig. 2C, top). The effect of soluble IL-9 treatment on CFSE-labeled wild-type B16F10 was also examined. Although a slight change was observed at 24 h after IL-9 treatment, the dramatic reduction, 2-fold, in CFSE fluorescence was noted at 48 h (Fig. 2C, bottom). To analyse the effect of IL-9 expression on B16F10 cell cycle, the sIL-9, mbIL-9, and mock transfected cells were fixed and stained with PI. As shown in Fig. 2D, IL-9 expression facilitated the cell cycling of B16F10 by increasing the portion of cells in S and G2/M phases at 1.6-fold each.

To further explore whether IL-9 has a role in cancer metastasis, which is an essential feature for malignant progression, the migration capability of transfectants was first examined by wound healing assay. The scratch areas from time points 0, 12, 24, 36 h are illustrated (Fig. 2E). The percentage of closed wound area indicated that sIL-9 or mbIL-9 expressing cells took 12 h to close in half and 36 h to completely close

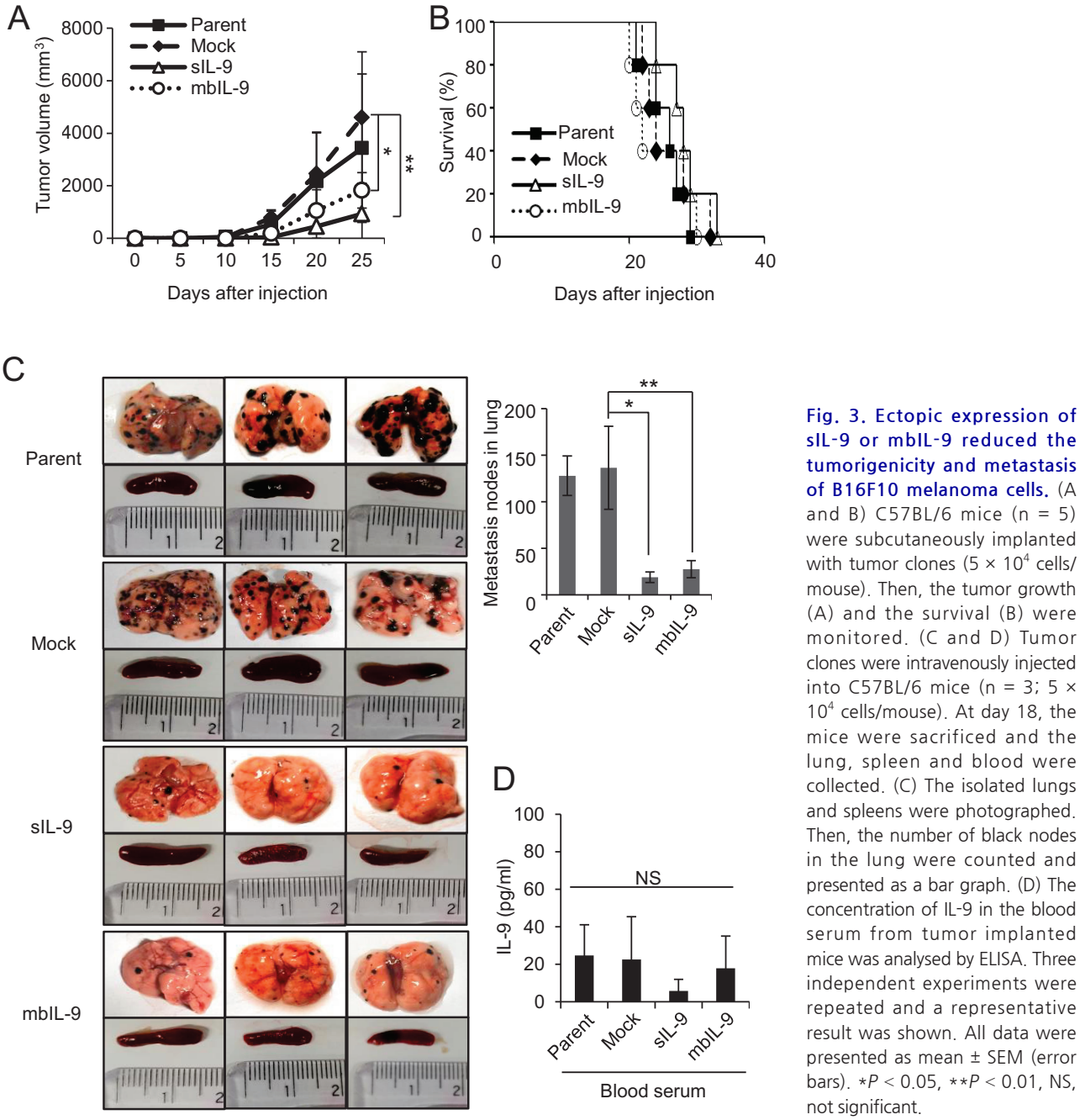

Fig. 3. Ectopic expression of sIL-9 or mbIL-9 reduced the tumorigenicity and metastasis of B16F10 melanoma cells. (A and B) C57BL/6 mice (n = 5) were subcutaneously implanted with tumor clones (5×10^4 cells/mouse). Then, the tumor growth (A) and the survival (B) were monitored. (C and D) Tumor clones were intravenously injected into C57BL/6 mice (n = 3; 5×10^4 cells/mouse). At day 18, the mice were sacrificed and the lung, spleen and blood were collected. (C) The isolated lungs and spleens were photographed. Then, the number of black nodes in the lung were counted and presented as a bar graph. (D) The concentration of IL-9 in the blood serum from tumor implanted mice was analysed by ELISA. Three independent experiments were repeated and a representative result was shown. All data were presented as mean ± SEM (error bars). $*P < 0.05$, $**P < 0.01$, NS, not significant.

the scratches, while cells from the control groups required 24 h to close in half the wound. Similar to wound healing assay, the increase in migration ability of sIL-9 or mbIL-9 transfectants was observed in the Transwell assay (Fig. 2F). The migration nodules at 48 h were increased to 18-fold and 12.9-fold in the sIL-9 or mbIL-9 groups, respectively, compared with the control groups. Our data clearly showed that ectopic expression of sIL-9 or mbIL-9 stimulated the migrating ability of B16F10 melanoma through the direct signalling of IL-9R on B16F10 cells.

Expression of sIL-9 or mbIL-9 delayed tumor growth and metastasis in mice

Although IL-9 expression exerted an autocrine effect on B16F10 cells as it promoted tumor proliferation *in vitro*, the influence of IL-9 in *in vivo* tumorigenesis remained elusive in our experimental condition. To evaluate the tumorigenesis of sIL-9 or mbIL-9 expressing clones, five mice were subcutaneously implanted with 5×10^4 cells of each tumor clones or control cells per mouse. Then the tumor growth and survival were monitored daily. As shown in Fig. 3A, the IL-9 expression reduced tumor growth as the tumor volume from the sIL-9 or mbIL-9 group was smaller than those from the mock control group in 5-fold or 2.5-fold at day 25 post-implantation, respectively. However, the ectopically expressing IL-9 failed to significantly extend the overall survival of tumor-bearing mice (Fig. 3B).

Next, we examined the effect of sIL-9 or mbIL-9 expression on *in vivo* metastasis capability of B16F10 melanoma. A metastasis model was set on groups of C57BL/6 mice (n = 3) by tail vein injection of 5×10^4 IL-9 expressing cells per mouse. Group of age-matched mice (n = 3) were intravenously injected with parent or mock-transfected cells as controls. Day 18 after the injection of tumor cells, the mice were sacrificed and their lungs, spleens, and blood were collected. On a macroscopic level, there was a significant decrease in the number of pulmonary metastatic nodules in sIL-9 and mbIL-9 groups for 7-fold and 5-fold, respectively, compared with the mock control (Fig. 3C). However, there was no difference in the sizes of spleen among mock control, sIL-9 and mbIL-9 cells and the concentration of IL-9 in the blood from all of the clones were in basal level (Figs. 3C and 3D). These results suggested that the intravenous implantation of sIL-9 or mbIL-9 expressing tumor clones did not alter the systemic IL-9 concentration, but the local expression of IL-9 inhibited tumor growth and metastasis in mice. Therefore, although IL-9 exerted the autocrine effect on B16F10 cells as promoting their proliferation (Fig. 2), it reduces the tumorigenesis of the cancer cells probably through stimulating the immune system *in vivo*.

IL-9 expressing cells stimulated the accumulation of M1 macrophages as well as T cells and NK cells in lung and spleen

We next examined which subsets of immune cells in mice participated in IL-9 mediated anti-tumor responses. After the mice were challenged as shown in Fig. 3C, the anti-tumor responses in the lung and spleen of tumor-bearing mice were analyzed at day 18. In the lung, as shown in Fig. 4A, the percentages of $CD4^+$, and $CD8^+$ T cell subsets increased up to 2.9-fold and 2.8-fold in both sIL-9 and mbIL-9 groups, respectively, compared to the mock control. In the case of NK cell population ($NK1.1^+CD49b^+$), the enhancement was also observed in sIL-9 and mbIL-9 in 1.7-fold and 2.2-fold, respectively. The most dramatic enhancement was observed in M1 macrophage population as the $CD80^+F4/80^+$, and $CD86^+F4/80^+$ population increased up to 4.4-fold and 4.3-fold in sIL-9 groups, respectively. For mbIL-9 groups, similar increases were observed. Interestingly, almost all of $F4/80^+$ cells from sIL-9 or mbIL-9 groups co-expressed NK1.1 on the cell surface as the $NK1.1^+F4/80^+$ population increased to 4.1-fold and 3.3-fold, respectively, compared to the mock control. These data suggest that M1 macrophage polarization driven by IL-9 might acquire some killer properties.

Similar trends were also observed in the spleen of IL-9 expressing tumor bearing mice. However, the differences in the percentage of $CD4^+$ T, $CD8^+$ T, NK cells, and M1 macrophages were less than 2-fold compared with the mock control. Furthermore, there was no change in splenic $NK1.1^+F4/80^+$ killer macrophage population (Fig. 4B).

IL-9 induced indirect anti-tumor immunity by stimulating the cytotoxic function of M1 macrophages

The *in vitro* immune stimulatory function of IL-9 was next investigated. Recently, the capability of IL-9 on stimulating cytotoxic function of T lymphocytes has been reported (Do Thi et al., 2018). In order to examine the effect of our IL-9 system on tumor eradicating ability of splenic lymphocytes, the spleen from mice immunized with MMC-treated B16F10 cells were collected. After the splenocytes were stimulated by co-culture with MMC-treated transfectants for 48 h, the cytotoxicity of the splenocytes against CFSE-labelled wild-type B16F10 was tested. As shown in Supplementary Fig. S1, at ratio 100:1, splenocytes stimulated with MMC-inactivated sIL-9 or mbIL-9 expressing cells triggered stronger anti-B16F10 cytotoxicity 1.8-fold than the mock control after 4 h of the co-incubation. Our result confirmed the role of IL-9 in inducing cytotoxicity of splenocytes.

Recently, M1 macrophages were reported to be associated with enhanced survival in lung cancer (Ma et al., 2010; Yuan et al., 2015). Since our FACS analysis for lung samples strongly suggested that IL-9 driven lung macrophages have potential anti-metastatic effect in B16F10 cells (Fig. 4A), the effect of IL-9 on *ex vivo* peritoneal macrophages and RAW264.7 macrophage cell line was further analysed. The peritoneal cells were isolated from mice, and the non-adherent cells were removed by washing with PBS and stimulated for 24 h by co-culture with either MMC-inactivated sIL-9, mbIL-9, or mock-transfected cells. The cytotoxic activities of the stimulated peritoneal macrophages against CFSE-labelled wild-type B16F10 were examined. As shown in Fig. 5A, in the ratio 4:1, peritoneal macrophages stimulated with MMC-inactivated sIL-9 or mbIL-9 expressing cells exerted higher anti-B16F10 cytotoxicity (2.2-fold) compared with controls after 4 h of the mixed-incubation. Furthermore, the addition of IL-9 culture supernatant enhanced the cytotoxic function of peritoneal macrophages for 1.7-fold compared with controls (Fig. 5B). The above data implied the potential role of IL-9 in the

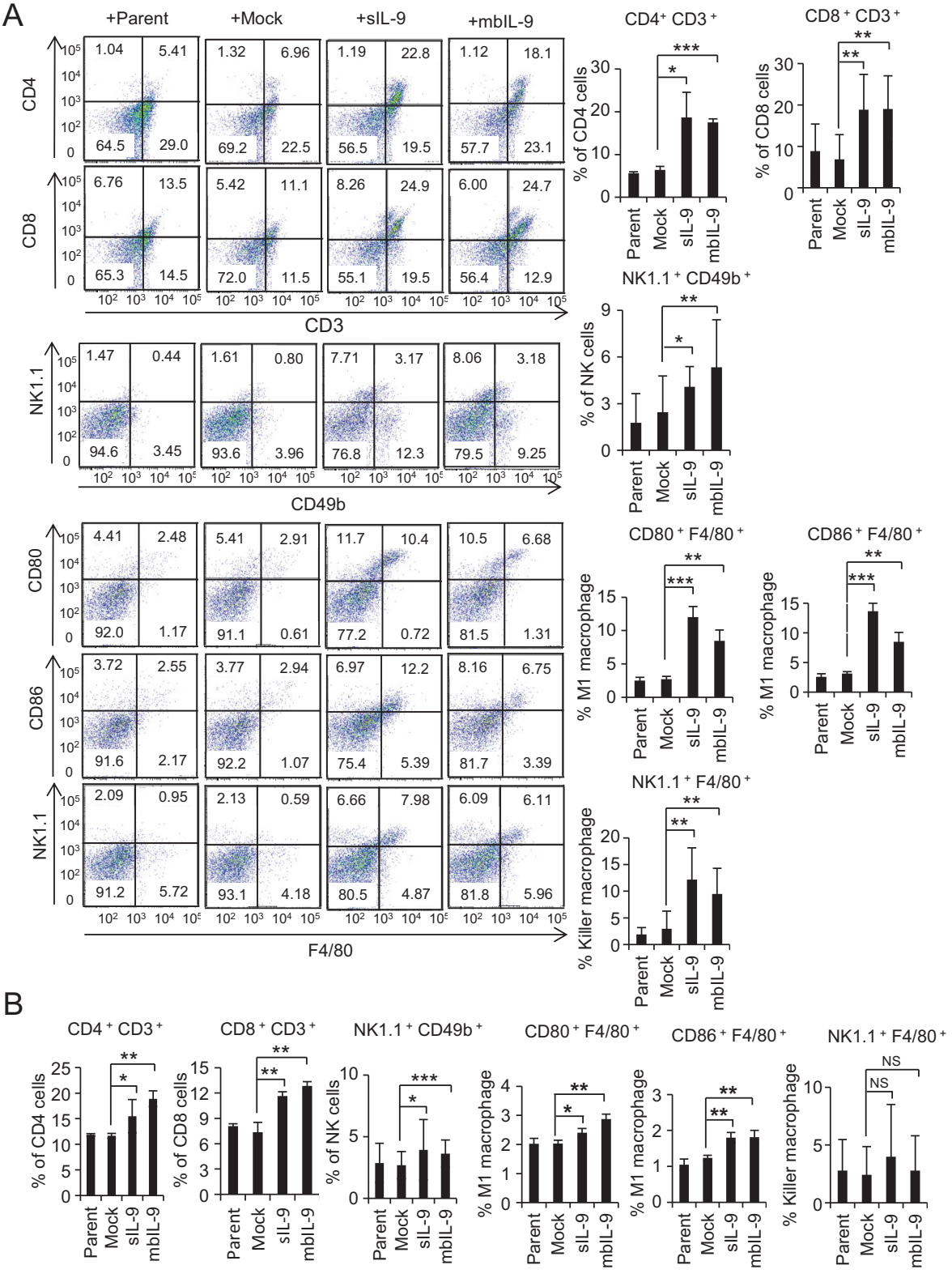

Fig. 4. Intravenous challenging with B16F10 clones expressing IL-9 stimulated the accumulation of CD4$^+$ T cells, CD8$^+$ T cells, NK cells and M1 macrophages in the lung and spleen of mice. The cells isolated from lung (A) or spleen (B) of tumor clones challenged mice described in Fig. 3C were stained and analysed for percentages of CD4$^+$ T cells (CD4$^+$CD3$^+$), CD8$^+$ T cells (CD8$^+$CD3$^+$), NK cells (NK1.1$^+$CD49b$^+$), M1 macrophages (NK1.1$^+$F4/80$^+$, CD80$^+$F4/80$^+$, CD86$^+$F4/80$^+$). The percentage of each population was graphed. All data were presented as mean ± SEM (error bars). $*P < 0.05$, $**P < 0.01$, $***P < 0.001$, NS, not significant.

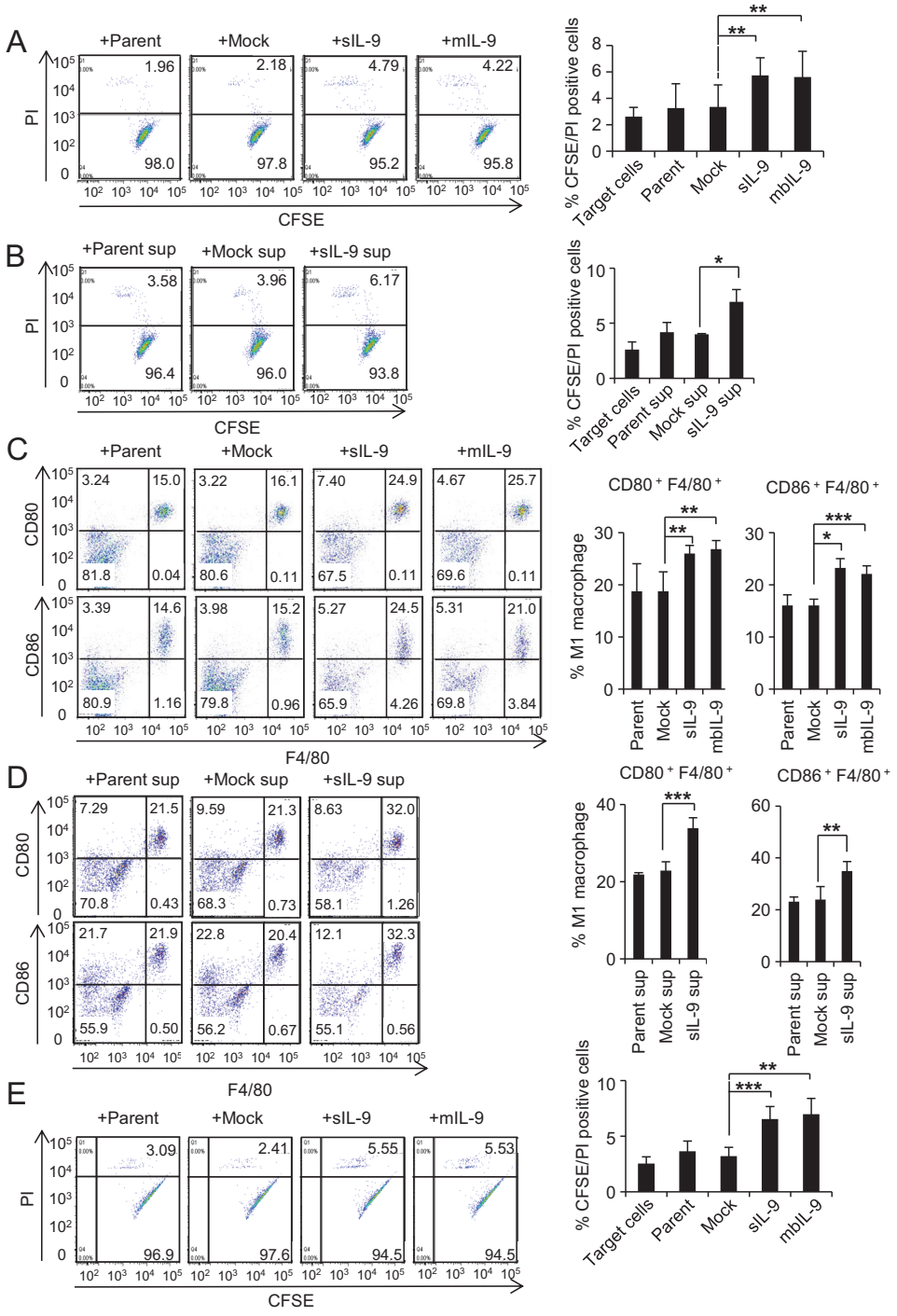

Fig. 5. IL-9 exerted its anti-tumor effect through stimulating cytotoxic activity of macrophages. (A) Peritoneal macrophages were stimulated with MMC-inactivated parent, mock, and IL-9 expressing B16F10 cells (ratio 1:1) for 24 h. The stimulated peritoneal macrophages were mixed-cultured with CFSE-labelled wild-type B16F10 cells at rate 4:1. After 4 h, the cell mixtures were harvested and stained with PI. Target cells; CFSE-labelled wild-type B16F10 cells only. (B) Peritoneal macrophages were stimulated with culture supernatant of IL-9-expressing B16F10 cells for 24 h. The stimulated peritoneal macrophages were mixed-cultured with CFSE-labelled wild-type B16F10 cells at ratio 4:1. After 4 h, the cell mixtures were harvested and stained with PI. (C) Peritoneal macrophages were stimulated as (A) for 24 h and analyzed by FACS staining with the indicated antibodies. (D) Peritoneal macrophages were stimulated as (B) for 24 h and analyzed by FACS staining with the indicated antibodies. (E) RAW264.7 cells were stimulated with MMC-inactivated IL-9 expressing B16F10 cells (ratio 1:1) for 24 h. The stimulated RAW264.7 was mixed-cultured with CFSE-labelled wild-type B16F10 cells at rate 4:1. After 4 h, the cell mixtures were harvested and stained with PI. All data were presented as mean ± SEM (error bars). $*P < 0.05$, $**P < 0.01$, $***P < 0.001$.

cytotoxic function of macrophages. To assess whether IL-9 can influence the polarization of macrophages, the surface markers of the stimulated peritoneal macrophages described in Fig. 5A were analyzed by FACS. As shown in Fig. 5C, the stimulation with MMC-inactivated sIL-9 or mbIL-9 expressing cells significantly enhanced M1 population ($CD80^+$ or $CD86^+$) of the macrophages in 1.6-fold compared with the control group. Similar data was observed in macrophages stimulated by IL-9 culture supernatant as the M1 population ($CD80^+$ or $CD86^+$) of macrophages from the treated group increased 1.4-fold compared to the control groups (Fig. 5D).

To further clarify the cytotoxicity of IL-9-stimulated macrophages, RAW264.7 murine macrophages were stimulated for 24 h with MMC-inactivated sIL-9, mbIL-9, or mock-transfected cells. Then, cytotoxic activities of the stimulated RAW264.7 against CFSE-labeled wild-type B16F10 were analysed. As shown in Fig. 5E, RAW246.7 cells stimulated with MMC-inactivated sIL-9 or mbIL-9 expressing cells exerted higher anti-B16F10 cytotoxicity (2.2-fold) compared with controls at 4 h after the co-incubation. Finally, RAW264.7 cells were treated with recombinant IL-9 (rIL-9) and compared with culture supernatants from IL-9 expressing clones. Treatment with 0.3 ng/ml rIL-9 enhanced the antitumor activity (1.8-fold), which is comparable to the effect of the culture supernatant from sIL-9 clone (2.3-fold) (Supplementary Fig. S2A). The portions of $CD80^+$ and $CD86^+$ RAW264.7 cells were clearly enhanced around 1.3 to 2.2 fold after treatment with rIL-9 and supernatant from sIL-9 clone (Supplementary Fig. S2B). Notably, the expression of IL-9R on both peritoneal and RAW264.7 macrophages were confirmed as shown in Supplementary Fig. S3. Taken together, our results revealed the new function of IL-9 as a potent anti-metastatic agent, in that IL-9 enhanced anti-tumor cytotoxicity by stimulating polarization to M1 macrophages.

DISCUSSION

Controversial function of IL-9 on tumor growth, in both promoting and inhibiting tumor progression were recently reported (Do Thi et al., 2018; Fang et al., 2015; Lee et al., 2019; Wang et al., 2019). However, circumstances that lead to pro-tumor or anti-tumor effect of IL-9 are still elusive. In this study, we showed that IL-9 exerts its direct effects on facilitating melanoma cancer cell division and metastasis. We also proved that IL-9 exerts its indirect anti-tumor effect by polarizing macrophages to M1 and stimulating the cytotoxic function of the macrophages.

To explore the effect of IL-9 in tumorigenesis progress of an IL-9Rα positive melanoma, we genetically engineered B16F10 melanoma cells to express either secretory or mbIL-9. sIL-9 and mbIL-9 was well detected either in culture supernatants or on the cell surface of the transfectants (Figs. 1C and 1E). The function of chimeric mbIL-9 in the biological assay was as efficient as the natural sIL-9 (Fig. 1F). To analyse the direct effect of ectopic IL-9 in transfected tumor cells, their abilities to proliferate and migrate *in vitro* were compared with control cells (Fig. 2). Surprisingly, ectopic IL-9-expression promoted *in vitro* growth by facilitating their cell cycle (Figs. 2A, 2C, and 2D) and enhanced migrating features of B16F10 transfectants (Figs. 2E and 2F). We asked if IL-9 itself exerted any direct effect on wild-type B16F10 cells, and found that the treatment with sIL-9 did promote the growth rate of wild-type B16F10 cells (Figs. 2B and 2C). These findings are consistent with several reports that IL-9 can serve as a mitogen for tumor cells (Hsieh et al., 2016; Ye et al., 2012). Our results presented that IL-9 exerted its autocrine effect via IL-9R mediated signaling to speed up the cell cycle of B16F10 cells. In a previous report, treatment with recombinant IL-9 exerted a pro-apoptotic effect on HTB-72 melanoma cell line (Fang et al., 2015). IL-9R complex may be a key to explain the contradictory effect of IL-9 on promoting or inhibiting cell growth in different melanoma cell lines.

Although the ectopic expression of IL-9 promoted *in vitro* proliferation and migration of the B16F10 transfectants, IL-9 expression successfully inhibited the cell growth and metastasis in C57BL/6 mice (Fig. 3). No significant toxicity was observed in mice implanted with sIL-9 or mbIL-9 transfectants (Supplementary Fig. S4). In an effort to investigate which subsets of immune cells were responsible for *in vivo* anti-metastasis effects of IL-9 in our experimental system, the common immune cells from the lung and spleen of tumor-bearing mice were characterized. As consistent with other reports (Do Thi et al., 2018; Kim et al., 2015; Lu et al., 2014b), $CD4^+$ T cells, and $CD8^+$ T cells were increased in lung and spleen of sIL-9 or mbIL-9 injected mice (Fig. 4). IL-9 can induce the activation of cytotoxic $CD8^+$ T cells (CTL) by provoking CTL favorable inflammatory tumor microenvironment and its homing to tumor sites (Lu et al., 2012). Since the IL-9 inducing CTL behaved differently compared to the conventional CTL, the new term, Tc9, was introduced to describe them (Lu et al., 2012; 2014a; 2014b). The effect of IL-9 on NK cell was previously reported as the disruption of IL-9 exerted a partial abrogation of NK cell development (Lanier, 2003). In our experimental model, the increase in NK ($NK1.1^+/CD49b^+$) population was also observed in the lung and spleen of sIL-9 or mbIL-9 injected mice. Since B16F10 cells do not express MHC class I (Supplementary Fig. S5), it can be anticipated that B16F10 cell line is a good target for the killer function of NK cells.

Interestingly, we found out a new responder candidate for IL-9. M1 macrophage population increased in the lung and spleen of sIL-9 or mbIL-9 transfectants-implanted mice (Fig. 4). Notably, a population which has surface markers from both macrophage and NK cells ($NK1.1^+F4/80^+$), was specifically increased in lung samples from sIL-9 or mbIL-9 groups (Fig. 4A). Our finding is in line with the previous report about the NK1.1-dependent tumor-killing effect of macrophages (Steiger et al., 2015). The impact of IL-9 on macrophages and splenic cells was further confirmed. IL-9 enhanced *in vitro* anti-B16F10 cytotoxic function of not only splenocytes but also of macrophages including RAW264.7 macrophages and *ex vivo* peritoneal macrophages (Fig. 5, Supplementary Fig. S1). We also proved that the stimulation of macrophages with IL-9 induced polarizing to M1 macrophage *in vitro* (Figs. 5C and 5D, Supplementary Fig. S2).

Lungs are surrounded by a large and compacted vascular area, so they are susceptible to cancer metastasis (Mukaida et al., 2018). Since lung tissues contain abundant blood

monocytes and tissue-resident macrophages, especially alveolar macrophages, the potent role of the macrophage in lung cancer progress has been recently reported (Mukaida et al., 2018; Tan and Krasnow, 2016). Macrophages are very plastic cells which can play diverse function depending on the microenvironment condition. The balance between M1 and M2 macrophages in tumor-associated macrophages decides the outcome of macrophages responses. M1 is a classically activated population of macrophage responsible for immunostimulatory functions to eliminate tumors (Conway et al., 2016; Mukaida et al., 2018). The presence of M1 macrophage in tumor microenvironment associated with better prognosis (Edin et al., 2012; 2013; Orecchioni et al., 2019), and the blockage of M2 polarization can inhibit the growth and migration of lung cancer (Xu et al., 2018). The activation of tumor-associated macrophages to the M1 phenotype can significantly delay tumor growth (Liu et al., 2015). Although the lack of direct evidence for anti-tumor cytotoxicity of macrophages has limited the clinical application of macrophages, the capability of macrophages to trigger anti-tumor cytotoxicity by releasing anti-cancer cytokines has been proven *in vitro* (Kaushik et al., 2019; Mantovani and Sica, 2010; Steiger et al., 2015). Here, we provided the first evidence of IL-9 driven macrophages as anti-tumor killer cells. The IL-9-driven macrophages showed killer phenotype as they expressed NK cell marker NK1.1 receptor (Fig. 4A). Those macrophages were also found to express M1 marker CD80 and CD86 (Figs. 4A, 5C, and 5D, Supplementary Fig. S2B). The direct anti-tumor cytotoxicity of the IL-9-driven M1 macrophages was also confirmed *in vitro* (Fig. 5, Supplementary Fig. S2A). Our results suggested that the potency of IL-9 for polarizing of lung macrophages to M1 population can be a new tool for cancer immunotherapy.

Note: Supplementary information is available on the Molecules and Cells website (www.molcells.org).

ACKNOWLEDGMENTS

This research was supported by the National Research Foundation of Korea (NRF) (2016R1D1A3B03934412) and by a grant from Chungnam National University.

AUTHOR CONTRIBUTIONS

Y.S.K. conceived experiments, wrote the manuscript, and secured funding. H.L., S.M.P., and V.A.D.T. performed experiments and wrote the manuscript. Y.S.K. and J.O.L. provided expertise and feedback.

CONFLICT OF INTEREST

The authors have no potential conflicts of interest to disclose.

ORCID

Sang Min Park https://orcid.org/0000-0001-7144-8230
Van Anh Do-Thi https://orcid.org/0000-0003-4670-6386
Jie-Oh Lee https://orcid.org/0000-0001-6519-6049
Hayyoung Lee https://orcid.org/0000-0002-8163-2880
Young Sang Kim https://orcid.org/0000-0002-2360-2595

REFERENCES

Chakraborty, S., Kubatzky, K.F., and Mitra, D.K. (2019). An update on interleukin-9: from its cellular source and signal transduction to its role in immunopathogenesis. Int. J. Mol. Sci. *20*, e2113.

Chang, H.C., Sehra, S., Goswami, R., Yao, W., Yu, Q., Stritesky, G.L., Jabeen, R., McKinley, C., Ahyi, A.N., Han, L., et al. (2010). The transcription factor PU.1 is required for the development of IL-9-producing T cells and allergic inflammation. Nat. Immunol. *11*, 527-534.

Ciccia, F., Guggino, G., Rizzo, A., Manzo, A., Vitolo, B., La Manna, M.P., Giardina, G., Sireci, G., Dieli, F., Montecucco, C.M., et al. (2015). Potential involvement of IL-9 and Th9 cells in the pathogenesis of rheumatoid arthritis. Rheumatology (Oxford) *54*, 2264-2272.

Conway, E.M., Pikor, L.A., Kung, S.H., Hamilton, M.J., Lam, S., Lam, W.L., and Bennewith, K.L. (2016). Macrophages, inflammation, and lung cancer. Am. J. Respir. Crit. Care Med. *193*, 116-130.

Dantas, A.T., Marques, C.D., da Rocha Junior, L.F., Cavalcanti, M.B., Goncalves, S.M., Cardoso, P.R., Mariz Hde, A., Rego, M.J., Duarte, A.L., Pitta Ida, R., et al. (2015). Increased serum interleukin-9 levels in rheumatoid arthritis and systemic lupus erythematosus: pathogenic role or just an epiphenomenon? Dis. Markers *2015*, 519638.

Dardalhon, V., Awasthi, A., Kwon, H., Galileos, G., Gao, W., Sobel, R.A., Mitsdoerffer, M., Strom, T.B., Elyaman, W., Ho, I.C., et al. (2008). IL-4 inhibits TGF-beta-induced Foxp3+ T cells and, together with TGF-beta, generates IL-9+ IL-10+ Foxp3(-) effector T cells. Nat. Immunol. *9*, 1347-1355.

Do Thi, V.A., Jeon, H.M., Park, S.M., Lee, H., and Kim, Y.S. (2019). Cell-based IL-15:IL-15Ralpha secreting vaccine as an effective therapy for CT26 colon cancer in mice. Mol. Cells *42*, 869-883.

Do Thi, V.A., Park, S.M., Lee, H., and Kim, Y.S. (2016). The membrane-bound form of IL-17A promotes the growth and tumorigenicity of colon cancer cells. Mol. Cells *39*, 536-542.

Do Thi, V.A., Park, S.M., Lee, H., and Kim, Y.S. (2018). Ectopically expressed membrane-bound form of IL-9 exerts immune-stimulatory effect on CT26 colon carcinoma cells. Immune Netw. *18*, e12.

Edin, S., Wikberg, M.L., Dahlin, A.M., Rutegard, J., Oberg, A., Oldenborg, P.A., and Palmqvist, R. (2012). The distribution of macrophages with a M1 or M2 phenotype in relation to prognosis and the molecular characteristics of colorectal cancer. PLoS One *7*, e47045.

Edin, S., Wikberg, M.L., Oldenborg, P.A., and Palmqvist, R. (2013). Macrophages: good guys in colorectal cancer. Oncoimmunology *2*, e23038.

Fang, Y., Chen, X., Bai, Q., Qin, C., Mohamud, A.O., Zhu, Z., Ball, T.W., Ruth, C.M., Newcomer, D.R., Herrick, E.J., et al. (2015). IL-9 inhibits HTB-72 melanoma cell growth through upregulation of p21 and TRAIL. J. Surg. Oncol. *111*, 969-974.

Goswami, R. and Kaplan, M.H. (2011). A brief history of IL-9. J. Immunol. *186*, 3283-3288.

Hsieh, T.H., Hsu, C.Y., Tsai, C.F., Chiu, C.C., Liang, S.S., Wang, T.N., Kuo, P.L., Long, C.Y., and Tsai, E.M. (2016). A novel cell-penetrating peptide suppresses breast tumorigenesis by inhibiting beta-catenin/LEF-1 signaling. Sci. Rep. *6*, 19156.

Kaushik, N.K., Kaushik, N., Adhikari, M., Ghimire, B., Linh, N.N., Mishra, Y.K., Lee, S.J., and Choi, E.H. (2019). Preventing the solid cancer progression via release of anticancer-cytokines in co-culture with cold plasma-stimulated macrophages. Cancers (Basel) *11*, e842.

Kim, I.K., Kim, B.S., Koh, C.H., Seok, J.W., Park, J.S., Shin, K.S., Bae, E.A., Lee, G.E., Jeon, H., Cho, J., et al. (2015). Glucocorticoid-induced tumor necrosis factor receptor-related protein co-stimulation facilitates tumor regression by inducing IL-9-producing helper T cells. Nat. Med. *21*, 1010-1017.

Lanier, L.L. (2003). Natural killer cell receptor signaling. Curr. Opin. Immunol. *15*, 308-314.

Lee, J.E., Zhu, Z., Bai, Q., Brady, T.J., Xiao, H., Wakefield, M.R., and Fang, Y. (2019). The role of interleukin-9 in cancer. Pathol. Oncol. Res. 2019 Apr 23 [Epub]. https://doi.org/10.1007/s12253-019-00665-6.

Li, H., Nourbakhsh, B., Cullimore, M., Zhang, G.X., and Rostami, A. (2011). IL-9 is important for T-cell activation and differentiation in autoimmune inflammation of the central nervous system. Eur. J. Immunol. *41*, 2197-2206.

Liu, M., Luo, F., Ding, C., Albeituni, S., Hu, X., Ma, Y., Cai, Y., McNally, L., Sanders, M.A., Jain, D., et al. (2015). Dectin-1 activation by a natural product beta-glucan converts immunosuppressive macrophages into an M1-like phenotype. J. Immunol. *195*, 5055-5065.

Lu, Y., Hong, B., Li, H., Zheng, Y., Zhang, M., Wang, S., Qian, J., and Yi, Q. (2014a). Tumor-specific IL-9-producing CD8+ Tc9 cells are superior effector than type-I cytotoxic Tc1 cells for adoptive immunotherapy of cancers. Proc. Natl. Acad. Sci. U. S. A. *111*, 2265-2270.

Lu, Y., Hong, S., Li, H., Park, J., Hong, B., Wang, L., Zheng, Y., Liu, Z., Xu, J., He, J., et al. (2012). Th9 cells promote antitumor immune responses in vivo. J. Clin. Invest. *122*, 4160-4171.

Lu, Y., Wang, Q., and Yi, Q. (2014b). Anticancer Tc9 cells: long-lived tumor-killing T cells for adoptive therapy. Oncoimmunology *3*, e28542.

Ma, J., Liu, L., Che, G., Yu, N., Dai, F., and You, Z. (2010). The M1 form of tumor-associated macrophages in non-small cell lung cancer is positively associated with survival time. BMC Cancer *10*, 112.

Malka, Y., Hornakova, T., Royer, Y., Knoops, L., Renauld, J.C., Constantinescu, S.N., and Henis, Y.I. (2008). Ligand-independent homomeric and heteromeric complexes between interleukin-2 or -9 receptor subunits and the gamma chain. J. Biol. Chem. *283*, 33569-33577.

Mantovani, A. and Sica, A. (2010). Macrophages, innate immunity and cancer: balance, tolerance, and diversity. Curr. Opin. Immunol. *22*, 231-237.

Mudter, J., Amoussina, L., Schenk, M., Yu, J., Brustle, A., Weigmann, B., Atreya, R., Wirtz, S., Becker, C., Hoffman, A., et al. (2008). The transcription factor IFN regulatory factor-4 controls experimental colitis in mice via T cell-derived IL-6. J. Clin. Invest. *118*, 2415-2426.

Mukaida, N., Nosaka, T., Nakamoto, Y., and Baba, T. (2018). Lung macrophages: multifunctional regulator cells for metastatic cells. Int. J. Mol. Sci. *20*, 116.

Nalleweg, N., Chiriac, M.T., Podstawa, E., Lehmann, C., Rau, T.T., Atreya, R., Krauss, E., Hundorfean, G., Fichtner-Feigl, S., Hartmann, A., et al. (2015). IL-9 and its receptor are predominantly involved in the pathogenesis of UC. Gut *64*, 743-755.

Orecchioni, M., Ghosheh, Y., Pramod, A.B., and Ley, K. (2019). Macrophage polarization: different gene signatures in M1(LPS+) vs. classically and M2(LPS-) vs. alternatively activated macrophages. Front. Immunol. *10*, 1084.

Steiger, S., Kuhn, S., Ronchese, F., and Harper, J.L. (2015). Monosodium urate crystals induce upregulation of NK1.1-dependent killing by macrophages and support tumor-resident NK1.1+ monocyte/macrophage populations in antitumor therapy. J. Immunol. *195*, 5495-5502.

Tan, S.Y. and Krasnow, M.A. (2016). Developmental origin of lung macrophage diversity. Development *143*, 1318-1327.

Wang, J., Sun, M., Zhao, H., Huang, Y., Li, D., Mao, D., Zhang, Z., Zhu, X., Dong, X., and Zhao, X. (2019). IL-9 exerts antitumor effects in colon cancer and transforms the tumor microenvironment in vivo. Technol. Cancer Res. Treat. *18*, 1533033819857737.

Xu, F., Cui, W.Q., Wei, Y., Cui, J., Qiu, J., Hu, L.L., Gong, W.Y., Dong, J.C., and Liu, B.J. (2018). Astragaloside IV inhibits lung cancer progression and metastasis by modulating macrophage polarization through AMPK signaling. J. Exp. Clin. Cancer Res. *37*, 207.

Ye, Z.J., Zhou, Q., Yin, W., Yuan, M.L., Yang, W.B., Xiong, X.Z., Zhang, J.C., and Shi, H.Z. (2012). Differentiation and immune regulation of IL-9-producing CD4+ T cells in malignant pleural effusion. Am. J. Respir. Crit. Care Med. *186*, 1168-1179.

You, F.P., Zhang, J., Cui, T., Zhu, R., Lv, C.Q., Tang, H.T., and Sun, D.W. (2017). Th9 cells promote antitumor immunity via IL-9 and IL-21 and demonstrate atypical cytokine expression in breast cancer. Int. Immunopharmacol. *52*, 163-167.

Yuan, A., Hsiao, Y.J., Chen, H.Y., Chen, H.W., Ho, C.C., Chen, Y.Y., Liu, Y.C., Hong, T.H., Yu, S.L., Chen, J.J., et al. (2015). Opposite effects of M1 and M2 macrophage subtypes on lung cancer progression. Sci. Rep. *5*, 14273.